Spatial and temporal electroselection patterns in electric field stimulation of polarized luminescence from photosynthetic membrane vesicles

Yosef Rosemberg, Philip Rozen, Shmuel Malkin,* and Rafi Korenstein
Department of Physiology and Pharmacology, Sackler Faculty of Medicine, Tel Aviv University, 69978 Tel-Aviv; and
*Department of Biochemistry, The Weizmann Institute of Science, Rehovot, Israel

ABSTRACT Electroselection processes of charge recombination are manifested in the study of electric field induced polarized emission from photosynthetic membrane vesicles. The study explores the coupled spatial-temporal characteristics of electric field induced charge recombination by examining the dependence of the integrated polarized emission and the time dependent polarization on electric field strength. The experimental results were fitted to theoretical models by computer simulations employing empirical parameters. Simulation of the dependence of the integrated polarized components of emission on electric field strength, suggests field-dependent increased ratio between radiative and nonradiative rates of charge recombination. The observation that the initial polarization values are independent of electric field strength supports the assumption that electric field induced emission originates from the pole area and then spreads away from it towards the equator. The propagation rate of this electric field induced charge recombination from the pole area towards the equator is reflected by the decay of polarization which increases upon raising the electric field strength. Simulation of the polarization's decay, based on a calculated angle of 26.3 ± 0.4° between the transition moment of emission and the plane of the membrane, establishes coupled temporal spatial patterns of electroselection in intramembrane electron transfer invoked by exposing preilluminated photosynthetic vesicles to a homogeneous electric field.

INTRODUCTION

Electrophotoluminescence (EPL) is observed when exposing preilluminated photosynthetic vesicles to external electric fields. Since the discovery of EPL (Arnold and Azzi, 1971) its study was used to probe, on the one hand, the photosynthetic apparatus and, on the other hand, to explore the mode of interaction of an external electric field with a vesicular membrane. Thus, by examining EPL, two independent electrophotoluminescence signals could be associated with photosystem I (PS I) and phtosystem II (PS II) (Symons et al., 1984; Symons et al., 1985; Vos and van Gorkom, 1988). The study of EPL revealed some thermodynamic features of electron transport in PS I and PS II (van Gorkom et al., 1986; Vos and Van Gorkom, 1988, 1990) and established the electrophoretic and diffusional mobilities of PS I in the photosynthetic membrane (Brumfeld et al., 1989). By using the EPL as an intrinsic voltage-sensitive optical probe, the electrical properties of the photosynthetic membrane were examined (Farkas et al., 1984), electroporation characteristics of the photosynthetic membrane were explored (Farkas et al., 1984a; Korenstein et al., 1984; Rosemberg and Korenstein, 1990a), and ionophore mediated ion transport was studied (Farkas et al., 1982; Rosemberg and Korenstein, 1990b).

The EPL phenomenon is explained by an electric field induced enhancement of charge recombination which leads to the creation of the singlet excited state of the specified chlorophyll pair of the primary electron donor. The excited primary donor may emit or lead to the creation of a singlet excited state in the pigment antenna system by energy transfer. These excited states are the emitters of EPL. Preillumination of a suspension of swollen thylakoid spherical vesicles leads to radially symmetrical vectorial charge separation (i.e., across the membrane, along the radius vector to a point on the membrane) in the protein complexes of the photosystems that are assumed to be homogeneously distributed in the vesicular membrane (scheme 1). Exposure of the preilluminated vesicles to a homogeneous external electric field leads to the induction of a local electric field in the membrane. The induced local electric field (E_m) in the membrane, upon exposure to an external electric field, has been calculated for spherical vesicles by solving Laplace's equation with the appropriate boundary conditions (Farkas et al., 1984; Ehrenberg et al., 1987). For the particular case where the specific conductivities of the inner and outer media, (λ_i and λ_o, respectively) are equal and where the vesicle's radius (R) is much bigger than membrane thickness (d), the expression for the time dependent induced electric field (E_m) at a point in the membrane is given by:

$$E_m = \frac{3(R/d)\cos\theta E_{ex}}{2 + 3(R/d)\cdot(\lambda_m/\lambda_o)} \cdot (1 - e^{(-2\lambda o t/3RC_m)}), \qquad (1)$$

Address correspondence to Dr. R. Korenstein, Department of Physiology and Pharmacology, Sackler Faculty of Medicine, Tel Aviv University, 69978 Tel-Aviv, Israel.

where E_{ex} is the externally applied electric field intensity switched on at time zero, λ_m is the specific conductivity of the membrane, C_m is the specific capacitance of the membrane, and θ is the angle between the applied electric field direction and the radius vector of the vesicle to a certain point in the membrane where a local electric field is induced. Hence, the membranal electric field increases from zero to a steady value, which is dependent on the azimuthal angle θ, with a time constant of $2\lambda_o/3C_mR$. Considering also that $\lambda_m \ll \lambda_o$, one obtains the following simplified approximate expression for the steady-state electric field which is induced in the membrane:

$$E_m = 3/2(R/d) \cdot E_{ex} \cdot \cos\theta. \quad (2)$$

Thus, exposure of a membrane vesicle to a homogeneous external electric field will lead to the induction of a nonhomogeneous electric field in the membrane, having an angular dependence. This angular dependence of the induced electric field has been demonstrated previously (Gross et al., 1986; Ehrenberg et al., 1987; Kinoshita et al., 1988, Hibino et al., 1991). The induced electric field in the membrane is parallel to the photo-induced charge separation in the hemisphere facing the cathode and antiparallel to the photo-induced charge separation in the other hemisphere facing the anode (scheme 1). Therefore, whereas stabilization of charge separation is induced in the hemisphere facing the anode, destabilization of the charge separation is induced in the hemisphere facing the cathode, leading to the induction of increased charge recombination in this hemisphere. This causes an enhanced electric field stimulation of luminescence (EPL) only from one hemisphere. This situation leads to a spatial selection of charge recombination, where recombination is induced only in those locations in the membrane where the light induced electric dipole has a component parallel to the induced electric field.

An additional constraint for charge recombination is reflected in the lag time of EPL appearance (Farkas et al., 1984). The lag time was attributed to the time needed to charge the membrane to an apparent threshold level of transmembrane potential difference ($\approx$240 mV), above which the EPL signal is detectable (Farkas et al., 1984). Since the EPL is time dependent and the time to reach a threshold for emission is dependent on electric field strength, the emission from different locations in the vesicular photosynthetic membrane is expected to occur at different times. Such a situation where a spatial-temporal selection of charge recombination is observed, may be attributed to a process of electroselection. Electroselection is a term previously coined by us (Farkas et al., 1980) to qualitatively explain the polarized emission of EPL. A more general definition of electroselection is its definition as a process that leads to the selection of a subset of induced chemical reactions, out of a large set of precursors for chemical reactions, according to the direction and amplitude of the local induced electric field. This notion of electroselection shares common features with the known photoselection process, where exposure of a randomly oriented set of molecules to a polarized light leads to the absorption of light only by the subset of molecules that have a component of their transition moment parallel to the electric vector of the polarized light.

This study presents a quantitative approach towards understanding the spatial and temporal electroselection patterns that govern the dependence of the EPL characteristics on electric field strength.

MATERIALS AND METHODS

Materials

Broken chloroplasts were prepared from spinach, pea, or tobacco according to Avron (1960). The broken chloroplasts were stored at −180°C in order to preserve their photosynthetic activity for a long period (Farkas and Malkin, 1979). In every set of experiments the concentrated thylakoids were thawed at room temperature and then incubated at 50°C for 3 min (heat activation) in order to deplete the thylakoids from most of their photosystem II related EPL activity, which depends less steeply on electric field strength (Symons et al., 1984), while preserving the photosystem I related activity (Symons et al., 1985). After heat inactivation the thylakoids were resuspended under hypotonic conditions. The concentration of the stored stock of broken thylakoids was 7 mg/ml, and they were diluted 300-fold in 5 mM MES-NaOH buffer pH 5.5 ($\sim 8 \times 10^6$ vesicles/ml). After 15 min at room temperature they were kept on ice. The swelling process, resulting from the hypotonic dilution, yields spherical vesicles known as "blebs." These vesicles, composed of a single membrane with occasional patches on it, have a size distribution of radii of 1–10 μm, with an average radius of 4 μm. The size distribution was determined by microscopic visualization. In order to further quench EPL related to photosystem II (PSII) and obtain EPL, which is associated mostly with photosystem I (PS I), the experiments were carried out in the presence of 50 μM tetraphenyl boron (TPB) (Sigma Chemical Co., St. Louis, MO), which was shown to abolish photosystem II associated EPL (Vos and van Gorkom, 1988). Alternative, we have also measured the difference of EPL in the absence and presence of 10 μM methyl viologen (Sigma Chemical Co.). Methyl viologen was shown to abolish photosystem I associated EPL (Symons et al., 1984, 1985, 1988).

Electrophotoluminescence studies

The experimental set-up for EPL measurements was described elsewhere (Farkas et al., 1984). The experiment was initiated by preillumination, for 120 ms. with a light projector. The light was filtered by a 4-96 glass filter (Corning Glass Works, Corning, NY) limiting the exciting wavelength range to ~400–600 nm. After a dark time of 20 ms an external electric field pulse was applied. The electric field pulse was delivered by a high voltage pulse generator (Velonex model 360; Santa Clara, CA), capable of delivering voltage pulses of 200–2,500 V. The applied voltage pulse shape, intensity, and kinetics were monitored by

the use of either a high voltage probe (model P6015; Tektronix Inc., Beaverton, OR) or by a pulse current transformer (model 411; Pearson Electronics, Palo Alto, CA). The electric field induced luminescence was filtered by a RG 665 cut-off filter (Schott Glass Technologies Inc., Duryea, PA), KS-DEM (Kasemann, Oberaudorf) polarizer and was monitored on a fast oscilloscope (model 2430A, Tektronix, Inc., Beaverton, OR) interfaced to a compatible IBM PC computer (Danbury, CT). All experiments were carried out at a temperature of 5°C maintained by a Techne RB-12 (Duxford, Cambridge) thermostated bath.

The parallel and perpendicular (in relation to electric field direction) polarized components of EPL were detected simultaneously by two photomultipliers (Hamamatsu R376; Bridgewater, NJ) forming a T configuration with the nonpolarized exciting light. Thus, if the direction of the electric field is parallel to the z-axis of the ordinary cartesian coordinate system and the polarizers are set in direction parallel to z and x-axes, the luminescence is viewed in the y-direction. The sample was preilluminated by a nonpolarized light through a light guide along the x-axis.

The polarization (p) of the electric field induced luminescence is defined by:

$$p = (I_{\parallel} - I_{\perp})/(I_{\parallel} + I_{\perp}), \tag{3}$$

where $I_{\parallel}$ and $I_{\perp}$ refer to the parallel and perpendicular polarized components of the electrophotoluminescence relative to the external field direction (scheme 1).

The contribution of the perpendicular and parallel polarized components of emissions from each element of the sphere is given by (Vos, 1990; Vos and van Gorkom, 1990):

$$I_{\parallel}(\theta) = I_t(-1/2 \sin^2\theta[3 \cos^2\alpha - 1] + \cos^2\alpha) \tag{4a}$$

$$I_{\perp}(\theta) = I_t(1/4 \sin^2\theta[3 \cos^2\alpha - 1] + 1/2 \cos^2\alpha), \tag{4b}$$

where α is the angle between the emission transition moment and the normal to the membrane plane at each site of the emitter, θ is the angle between the radius vector to the site of the emitter and the radius vector to the pole, and I_t is the total emission intensity per unit area.

For $\theta = 0°$ the relationship between a and the polarization p reduces to

$$0.5\, tg^2\alpha = (1 + p)/(1 - p). \tag{5}$$

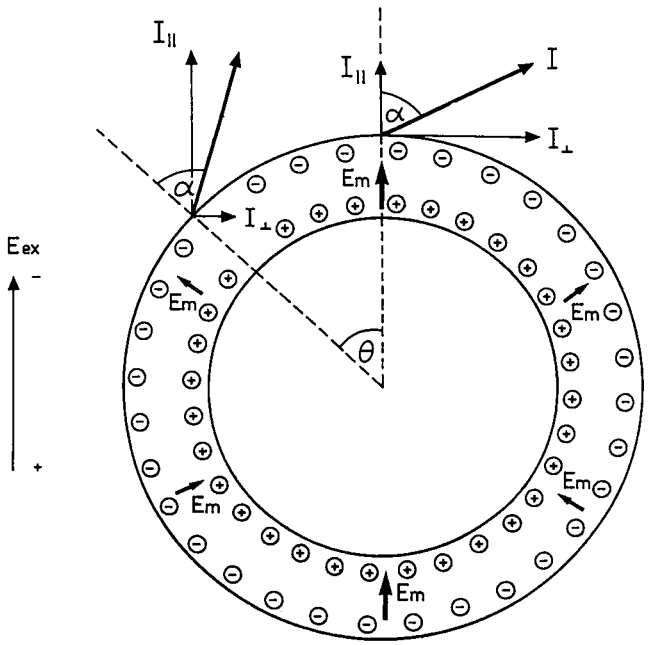

SCHEME 1 The scheme describes the angular dependence of the induced local electric field (E_m) upon exposure to an external electric field (E_{ex}) in relation to the radial distribution of the light induced charge separation (where the circles containing the "+" sign represent the oxidized donors and the circles containing the "−" sign represent the acceptors). The solid arrows in the membrane describe the amplitude and direction of E_m at different locations in the membrane. The transition moment of emission (I) forms an angle α with the normal to the membrane plane (shown by a discontinuous line). $I_{\perp}$ and $I_{\parallel}$ represent the perpendicular and parallel (relative to electric field direction) polarized components of the transition moment of emission. The decomposition of the transition moment into its polarized components is shown for two different locations in the membrane vesicle. It should be stressed that this scheme is only a two-dimensional model (describing only specific situations), whereas the real three dimensional situation for the components of polarization is given by Eqs. 4, *a* and *b*.

RESULTS AND DISCUSSION

Dependence of the initial polarization of electrophotoluminescence on electric field strength

The time dependent polarization of the EPL signal, following its rise, was calculated for each time point from the corresponding measured parallel and perpendicular components of the EPL (Fig. 1 *a* and *b*). The polarization was negative throughout the experiment with a maximal absolute value, initially. Since, in the initial rise phase of the EPL, the signal-to-noise ratio is low, there exists some ambiguity with regard to the polarization values of the very initial points in the EPL rise curve, especially for the EPL recorded at low electric field strength. The entire data points of the time dependent polarization were best fitted by a sum of two exponents. The initial values of polarization were obtained from extrapolation of data points closest to the initial part of the fitted curve. The initial polarizations, measured at different external electric fields show independence on the electric field strength (Fig. 2). This finding differs from our previous observation (Farkas et al., 1980) where the initial polarization was found to be dependent on electric field strength in the range of 800–1,500 V/cm. This discrepancy is attributed to the poor signal-to-noise obtained previously in the analysis process, based on oscilloscope photographs of the EPL traces rather than on analysis based on digitized data as was done in this study. During the charging process the induced electric field in the membrane increases from zero, attains the critical threshold value for emission,

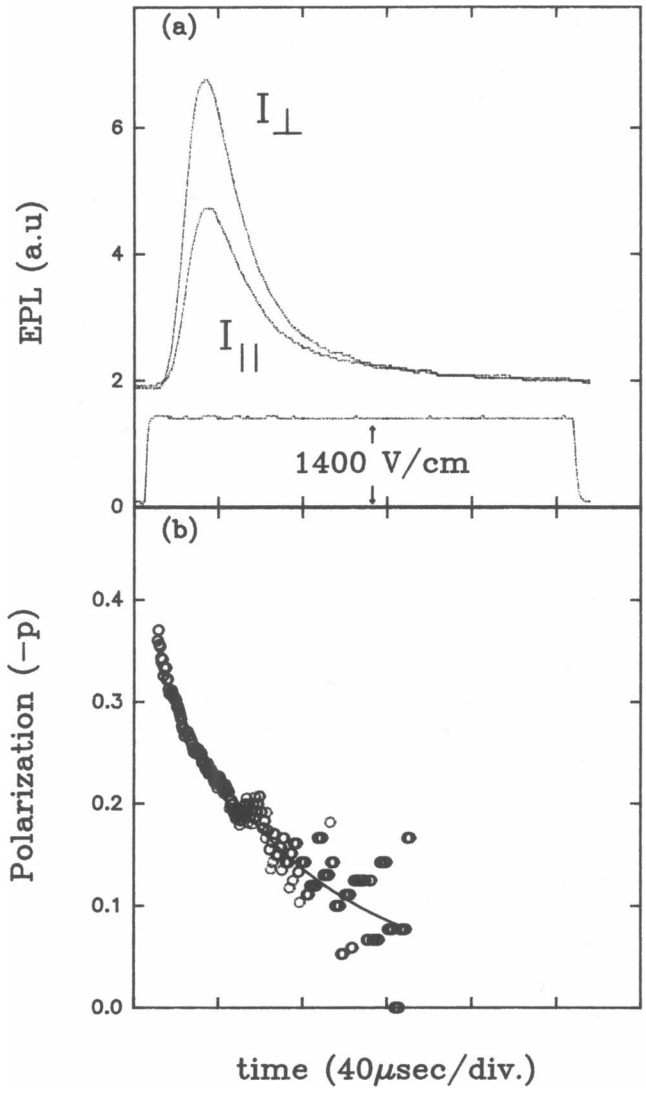

FIGURE 1 Polarization characteristics of electrophotoluminescence (EPL). EPL was measured from swollen thylakoids suspended in 5.5 mM Tris, 50 μM TPB, pH = 5.5, and exposed to external electric field of 1,400 V/cm. The electric field was applied 20 ms after the termination of a 120 ms preillumination. (*a*) Time dependent traces of the perpendicular ($I_\perp$) and parallel ($I_{||}$) polarized components of the EPL. The rectangular curve under the EPL traces is the shape of the applied voltage pulse. (*b*) Time dependent polarization values (*circles*) calculated from the polarized EPL components shown in *a*. The polarization values are negative (expressed as $-p$). The solid curve was obtained by fitting the data points to a sum of two exponents.

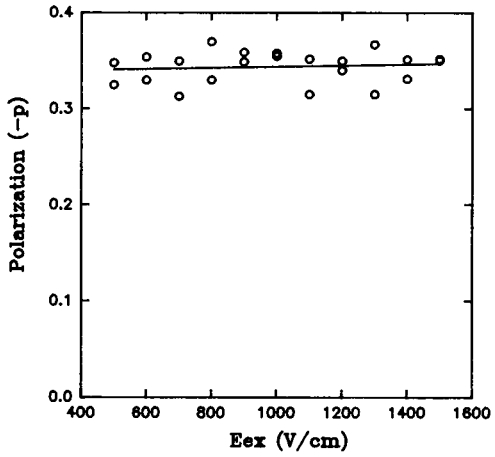

FIGURE 2 Dependence of the initial values of polarization on external electric field strength. The polarization values are negative (expressed as $-p$). The initial polarization was calculated from the two initial values of the parallel and perpendicular polarization components of EPL measured at different electric fields. The solid line represents a linear regression of the experimental points.

and continues to increase to a steady state value (Fig. 3). The threshold of the induced electric field strength in the vesicle will be established at first in the pole areas and only later at areas away from the pole as can be visualized from the theoretical curves, based on Eq. 1 (Fig. 3 *a*). Hence, we would expect to observe the initial polarization to originate from the pole area. Furthermore, from the theoretical curves of Fig. 3 *b* we would expect to obtain shortening of the lag time with the increase of the applied electric field. These arguments support the assumption that the initial polarization reflects emission from the pole area ($\theta = 0°$). Thus, the angle that the transition moment of emission forms with the membrane can be calculated by inserting the value of initial polarization in Eq. 5. An average initial polarization of -0.34 ± 0.02 was obtained when applying different external electric fields. The initial polarization values were insensitive to a fivefold change in the number of vesicles per unit volume, suggesting no attenuation of the initial polarization due to possible effects of static or dynamic light scattering. The obtained average initial polarization of 0.34 ± 0.02 yields an average value of $63.7 \pm 0.4°$ for α. Thus, the transition moment of emission forms an angle of $26.3 \pm 0.4°$ with the plane of the membrane. This value is similar to the value of 23° obtained by a different approach, based on the simulation of the time course of the polarized components of EPL (Vos, 1990; Vos and van Gorkom, 1990).

The dependence of the integrated polarized components electrophotoluminescence on electric field strength

The dependence of the integrated parallel and perpendicular components of PS I associated EPL (i.e., the integrated luminescence under the parallel and perpendicular EPL time curves) on the electric field strength

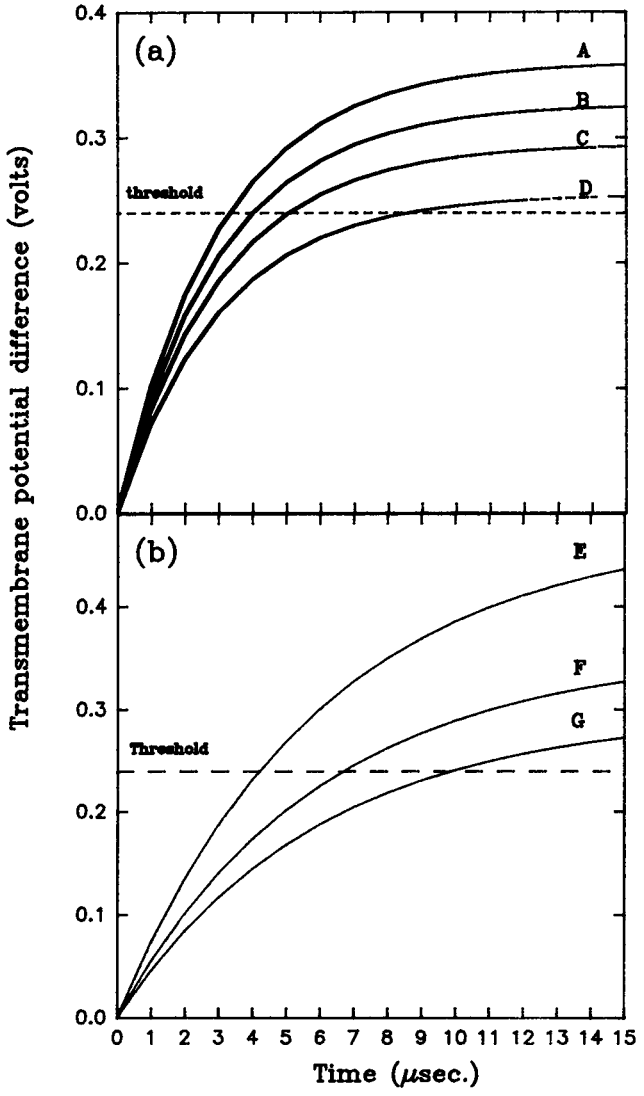

FIGURE 3 Simulation of the charging kinetics. The values of the transmembrane potential difference during the charging process were calculated by Eq. 1, where $\lambda_m = 170$ nS, $\lambda_o = 200$ μS, $R = 4$ μm, $d = 50$ nm, and $C_m = 1$ μF. The broken horizontal line (----) represents the 240 mV transmembrane potential difference threshold for emission. (*a*) The charging kinetics at four different locations in a membrane hemisphere defined by four different spatial angles (θ): 0° (*A*); 25° (*B*); 35° (*C*); 45° (*D*) when exposed to external electric field of 1,500 V/cm. (*b*) The charging kinetics in the pole area (θ = 0°) upon exposure to three different external electric fields of: 1,600 V/cm (*E*); 1,200 V/cm (*F*); 1,000 V/cm (*G*).

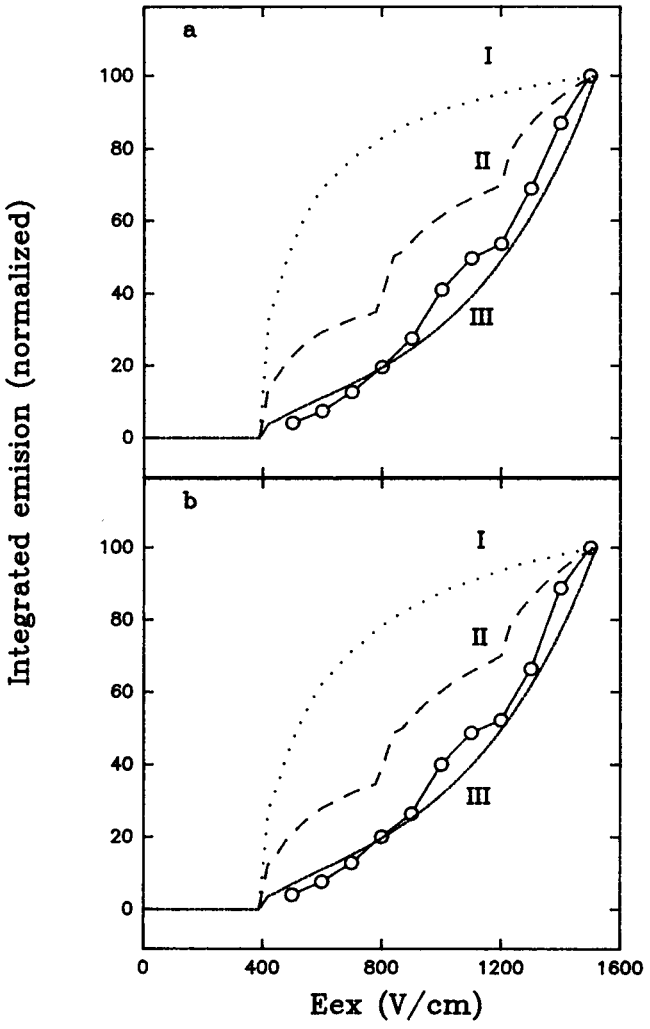

FIGURE 4 Dependence of the integrated parallel and perpendicular components of EPL on the external electric field strength (E_{ex}). The duration of exposure to the external electric field was 1 ms. Experimental data: open circles (—○—) connected by a solid line; simulation based on model I, small points (. . . .); simulation based on model II dashed line (- - -); simulation based on model III, small dashed line (---). (*a*) Simulation of the dependence of the integrated perpendicular component of EPL on electric field strength; (*b*) simulation of the dependence of the integrated parallel component of EPL on electric field strength.

(Fig. 4) was measured by applying long enough electric field pulses that finally lead to the total decay of the EPL signal. The exposure to electric fields was restricted to strength values $\leq 1{,}500$ V/cm to avoid a significant electroporation of the membrane (Rosemberg and Korenstein, 1990a). The dependence of the measured maximal values of the unpolarized EPL (EPL_{max}) on electric field strength is shown in Fig. 5.

The dependence of the integrated parallel and perpendicular components of EPL on electric field strength was calculated by three different models. The complexity of the phenomenon forced us to some approximate assumptions. The basic assumptions in all three models are:

(*a*) EPL is emitted only from those regions on a hemisphere where the induced local electric field in the

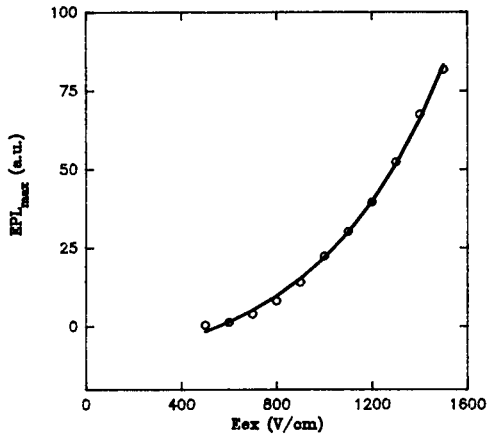

FIGURE 5 The dependence of the peak amplitude of EPL (EPL_{max}) on external electric field. The peak values, given by circles (○), were taken as the highest experimental values of the non-polarized EPL traces at the different electric fields. The dependence of EPL_{max} on the external electric field strength was fitted to a single exponent of the type $f(E_{ex}) = A \cdot e^{(K \cdot Eex + C)}$. The experimental conditions are identical to those in Fig. 1.

membrane has reached the apparent electric field threshold for emission (Farkas et al., 1984).

(*b*) All precursors of emission are distributed evenly in the membrane of the vesicle.

The region from which EPL is emitted (defined by a limiting azimuthal angle) was calculated from Eq. 2 by determining, for each electric field strength, a critical angle, θ^*, at which the induced local electric field is equal to the threshold level for emission. The region from which emission occurs is given by $\theta \leq \theta^*$.

In the first model (model I) we assume that the membrane contains precursors of emission that share a common electric field threshold of 4.8×10^5 V/cm (corresponding to a transmembrane potential difference of 240 mV) for emission (Farkas et al., 1984). Furthermore, we assume that during exposure to a long electric field pulse, all precursors of emission are depleted from those regions in the vesicle's hemisphere where the induced local electric field is equal to or greater than the electric field threshold for emission. The simulation of the integrated intensity of the polarized components of EPL starts by calculating from Eq. 2 the critical angle, θ^*, for each value of electric field strength. The integrated intensity emitted at a specified external electric field strength, is calculated by integrating each of the polarized emission components, I_{pol}, (which represents either $I_\perp$ or $I_\parallel$) over $\theta \leq \theta^*$. Hence,

$$\text{integrated } EPL_{pol} = \int_0^{\theta^*} I_{pol}(\theta)\, d\theta, \qquad (6)$$

where $I_\parallel$ is given by Eq. 4 *a*, $I_\perp$ is given by Eq. 4 *b*, and I_t in Eqs. 4a and b was taken as unity. The simulations of the integrated parallel and perpendicular components of EPL (Fig. 4 *a*, curve I and Fig. 4 *b*, curve I, correspondingly) clearly differ from the experimental data points.

The second model (model II) assumes the existence of three populations of precursors, distributed with equal density in the vesicular membrane and possessing three different electric field thresholds for emission. Since there exist four electron acceptors in the membrane, (A_1, the primary acceptor, and three consequent iron-sulfur cluster acceptors F_X, F_A, and F_B (Murphy, 1986)), we assume that reverse electron transfer to the primary donor (P-700) from the three secondary acceptors is associated with three corresponding different electric field threshold levels for charge recombination. In addition, we assume that the values chosen for these thresholds are multiples of the experimentally determined threshold of model I, namely, induced electric fields of 4.8×10^5 V/cm, 9.6×10^5 V/cm and 1.4×10^6 V/cm (corresponding to transmembrane potential difference thresholds of 240, 480, and 720 mV). Since we assume the existence of different threshold values, when increasing electric field strength, we stimulate emission from additional population of emitters located in the same area from which emission is stimulated at a lower electric field. In this case the integrated polarized luminescence from a unit area defined by θ is equal to the sum of polarized emissions of the three different populations. The integrated intensity emitted at a specified electric field strength is calculated by summing up the three integrated polarized emission components. Hence,

$$\text{integrated } EPL_{pol} = \int_0^{\theta_1^*} I_{1,pol}(\theta)d\theta + \int_0^{\theta_2^*} I_{2,pol}(\theta)d\theta + \int_0^{\theta_3^*} I_{3,pol}(\theta)d\theta, \qquad (7)$$

where $I_1(\theta)$, $I_2(\theta)$, and $I_3(\theta)$ are emission intensities (given by Eqs. 4a and b) corresponding to three emitter populations and possessing three critical angles θ_1^*, θ_2^*, and θ_3^*, which correspond to the three different thresholds, at a specified external electric field strength. The dependence of the calculated integrated parallel and perpendicular polarized components of EPL on E_{ex}, based on model II, are given by curves II in Fig. 5, *a* and *b*, correspondingly. The calculated dependence clearly does not fit the experimental data. The shape of the calculated curves depends, of course, on the choice of the threshold values. However, other values of threshold that were tested did not improve the fit to the experimental data.

The third model (model III) assumes, as does model I, the existence of a single population of emitters possessing a single threshold value of 4.8×10^5 V/cm. The

assumption here is that the total amount of EPL originating from any single precursor depends on the local electric field strength. This means that the ratio between radiative and nonradiative processes, that take place during charge recombination in the photosynthetic membrane, changes with the strength of the externally applied electric field. Since the induced local electric field varies from point to point over the hemisphere, the contribution of I_t, the total emission intensity per unit area, will vary according to the local electric field. As a starting point for this model we assume that the functional dependence of I_t on E_{ex} follows the experimental dependence of the peak amplitude of EPL (EPL_{max}) on E_{ex}. The experimental dependence of EPL_{max} on the electric field strength is shown in Fig. 5. EPL_{max} was found to depend exponentially on the external electric field strength (Fig. 5). Thus, the integrated intensity emitted at a specified electric field strength, is calculated by integrating the polarized emission component, I_{pol} (which represents either $I_\perp$ or $I_\parallel$), over $\theta \leq \theta^*$. Hence,

$$\text{integrated } EPL_{pol} = \int_0^{\theta^*} I_{pol}(\theta)\, d\theta, \tag{8}$$

where $I_\parallel$ is given by Eq. 4 a, $I_\perp$ is given by Eq. 4b, and the dependence of I_t on electric field strength (over the range studied) was taken by fitting the data in Fig. 5, yielding an approximate functional dependence of:

$$I_t :: e^{(E_{ex}\, 0.0025 \cos\theta^*)}. \tag{9}$$

The dependence of the simulated integrated parallel and perpendicular polarized components of EPL on E_{ex}, based on model III, are given by curves III in Fig 5, *a* and *b*, correspondingly. The simulated dependence approaches closely the experimental one. Thus, only model III yields simulated curves, which are close to the experimental data.

Time-dependent polarization characteristics of electrophotoluminescence at different external electric fields

The dependence of the measured temporal polarization characteristics of the EPL on electric field strength is shown in Fig. 6, *a*, *c*, *e*. The time dependent polarization of the EPL signal (Fig. 6, *b*, *d*, *f*) was obtained, following its rise, for each time point, from the corresponding measured parallel and perpendicular components of emission (Fig. 6, *a*, *c*, *e*). Though the initial polarization was found to be field independent (Fig. 2) as was discussed above, its decay was found to increase upon raising electric field strength (Fig. 6, *b*, *d*, *f*). This is particularly evident from the increase in the initial rate of polarization decay upon elevating electric field strength (e.g., the initial decay was 2,400 s^{-1} at 800 V/cm, 3,600 s^{-1} at 1,000 V/cm, 4,500 s^{-1} at 1,200 V/cm, and 6,600 s^{-1} at 1,400 V/cm). This observation can be explained qualitatively by considering that the polarization of EPL becomes smaller for emission which originates from locations at a further distance from the pole area (scheme 1). The time for the local field to reach the threshold for emission in the pole area and in any other location away from it decreases for stronger external electric fields. Consequently, contributions from regions far away from the pole will materialize sooner with stronger external electric fields. Therefore, the polarization will decay faster at a higher electric field.

The simulation of the time dependent polarization characteristics of EPL is based on a semi-empirical approach. The polarization expected from any surface unit, located at angle θ (where the transition moment of emission forms an angle of $\alpha = 64°$ with the normal to the membrane plane) was calculated from the average value of initial polarization by Eq. 4. Different points on the hemisphere of a vesicle are assumed to reach threshold of emission at different times due to the angular dependence ($\cos\theta$) of the induced electric field (see Fig. 3 *a*). The rise of the stimulated emission appears to lag behind the application of the external electric pulse (Fig. 1). The dependence of the lag time on electric field strength (E_{ex}) was measured and is shown in Fig. 7. The obtained dependence of the lag time on the external electric field was fitted by the following expression:

$$t_{lag} = ae^{(-bE_{ex}/(E_{ex}+c))}, \tag{10}$$

where $a = 1.36\ 10^{28}$, $b = 63$, and $c = 27$. This expression enabled us to calculate the time needed to reach a threshold level for emission at a given point on the membrane hemisphere. The emission intensity of an emitter at any location on the hemisphere, assumed to depend on the strength of the induced electric field in that location (model III), was calculated by Eq. 9. The emission is assumed to start instantaneously after the membrane potential reaches a threshold, to grow rapidly to a maximum, and then decay exponentially. Again, a simplifying assumption must be made, that the decay rates of emission are obtained from the averaged experimental data of the observed EPL decay, after it reached its maximum (an average decay rate for different external electric fields). The decay rate could then be fitted by a single decay of the type of ae^{-kt}, where for the simulation we used the following average values: $a = 4.45$ and $k = 0.021\ \mu s^{-1}$. From this, the intensity of emission at any particular time point is given by:

$$I_\theta(t) = e^{0.0025 E_{ex} \cos\theta} \cdot 4.45e^{-0.021t}. \tag{11}$$

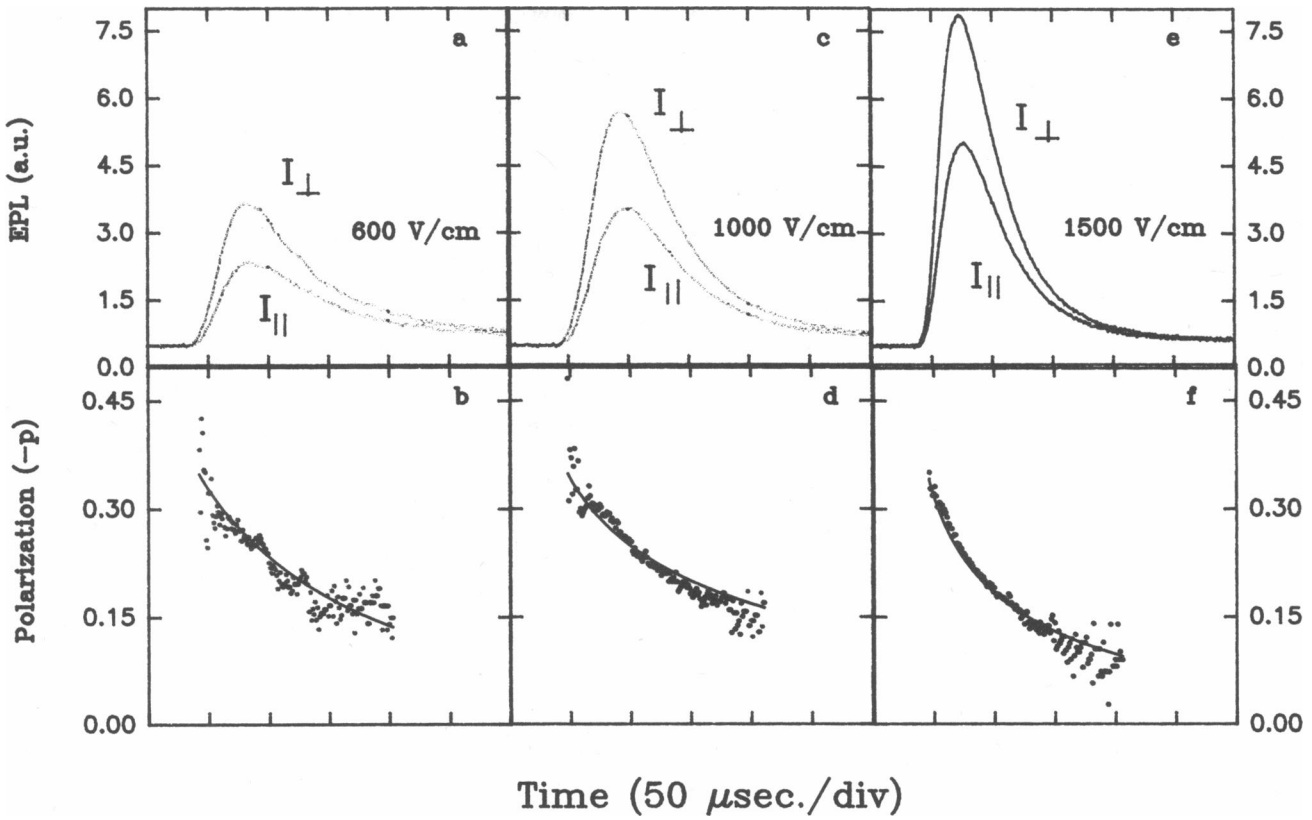

FIGURE 6 Time dependent polarization of electrophotoluminescence (EPL) at different external electric field strength. The perpendicular ($I_\perp$) and parallel ($I_\parallel$) polarized emission components of EPL were measured simultaneously at different external electric field strength. The time dependent polarized components of EPL are shown in *a*, *c*, and *e*. The corresponding calculated polarizations values (the polarization values are negative, expressed as $-p$) are shown as dots (.) in *b*, *d*, and *f*, respectively. The solid curves (——) in *b*, *d*, and *f* represent the calculated time-dependent polarization values from the semi-empirical model of polarization's decay based on model III. The calculation is based on using a value of $a = 64°$ and fitting the experimental data when the free parameter was the average radius of the swollen thylakoid population. The experimental conditions are identical to those in Fig. 1.

It follows from the above assumptions that precursors of emission, at a certain location in the membrane, are not depleted promptly when the local electric field at that location reaches the threshold level and that they decay exponentially with time. The observed polarization (p), at any particular time, is therefore an average one due to contributions of emissions associated with all those precursors that are induced to emit in the area enclosed by the critical angle, θ^*, at that particular time. Hence, the contribution of the different emitters to the observed average polarization will be given both by their intensity of emission (which depends on the local induced electric field (see model III)) and by their exponential decay with time. Based on the above assumptions the time dependent average polarization is calculated as the sum of the polarization values associated with all angles θ_i ($i = 0 \ldots n$, where $\theta_1 = 0°$ and $\theta_n = \theta^*$) multiplied by the corresponding emission intensities I_θ and divided by the sum of the corresponding intensities. Thus,

$$p_{\text{average}}(t) = \sum_{i=1}^{n} (p_{\theta_i} \cdot I_{\theta_i}) \Big/ \sum_{i=1}^{n} I_{\theta_i}. \tag{12}$$

Because of the size heterogeneity of the swollen thylakoid vesicles simulation was fitted to the experimental data by choosing an average radius. The simulation of the observed decay of polarization, at different electric fields, is shown in Fig. 6, *b*, *d*, *f*. It can be seen from Fig. 6 that the semi-empirical model, suggested for the temporal polarization characteristics of EPL, gives a good description of the experimental findings. These results reflect the spatial propagation of the electric field induced charge recombination from the pole area towards the equator as a function of electric field strength.

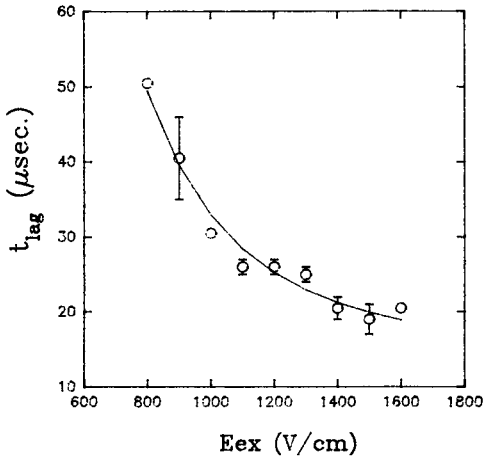

FIGURE 7 Dependence of the lag time (t_{lag}) on electric field strength (E_{ex}). The t_{lag} was determined at different strengths of the electric field (*circles*). Where no error bars are indicated the symbols are bigger than the standard deviation. The data points were fitted by a function of the type $t_{lag} = 1.36 \cdot 10^{28} \cdot e^{(-63E_{ex}/(E_{ex}+27))}$. Other experimental conditions were identical to those in Fig. 1.

CONCLUDING REMARKS

The polarization characteristics of EPL result from an electroselection process of intramembrane electron transfer reactions associated with PS I, which proceed across the membrane in a perpendicular direction to its plane. Electroselection is driven by an induced electric field which possesses both spatial and temporal characteristics. Under stationary conditions we expect to produce electroselection due to the spatial variation in amplitude and direction of the induced local electric field at different sites in the membrane hemisphere. Thus, if an electrogenic process can occur only in a direction perpendicular to the plane of a vesicular membrane, in the inside to outside direction, exposure of a vesicle to a homogeneous electric field will induce a chemical process only in one hemisphere, where the local induced electric field has a parallel component to an existing electric dipole in the membrane. Furthermore, electroselection possesses a coupled temporal-spatial character due to the charging process. Thus, when a threshold for an electric field induced process exists, the reaction will be induced by low electric fields first in the membrane regions whose normal is aligned very closely to the field direction (pole areas), and only with increasing field strength will regions away from the poles be electrically activated. The rate of the electroselection process, viewed as a propagation of electric field induced charge recombination from the pole area towards the equator, increases with electric field strength. These electroselection patterns should be taken into consideration when studying the effects of pulsed or oscillating external electric fields on membrane proteins in organelles and cells (Tsong and Astumian, 1987; Tsong 1989; Serpersu and Tsong 1983, 1984; Blank and Soo, 1990; Liu et al., 1990).

The dependence of the polarization characteristics of EPL on electric field strength reveal structural information on the orientation of the transition moment of PS I associated emission with the plane of the membrane. The transition moment of emission forms an angle of 26.3 ± 0.4° with the plane of the membrane. The molecular identity of the emitter is still unknown. After electric field induced charge recombination, a singlet excited state of the primary donor is created. The electronically excited donor can either emit this light or transfer it to the nearest antenna system associated with it. In the latter case the antenna will be the source of luminescence. Alternatively, one could assume energy transfer from the antenna associated with the primary donor to the antenna molecules of the light harvesting complex. However, in this case, due to the multiple orientations of the antenna molecules in the light harvesting complex, the resultant emission should be unpolarized. Thus, we may conclude that EPL emitters are either the specified chlorophyll pairs of the primary electron donor of PS I or a highly ordered PS I associated pigment antenna system. Another conclusion from this study is the suggestion that the ratio between radiative and nonradiative processes, that take place during charge recombination in the photosynthetic membrane, increases exponentially with the strength of the induced electric field. This could be due to the different sensitivities of the three possible recombination paths to the electric field recombinations that lead to the singlet or triplet excited state or a recombination which leads directly to the ground state.

We thank Israel Miller and Dov Lichtenberg for helpful discussions. This work was carried out in partial fulfillment of a Ph.D. thesis requirement of Y. Rosemberg.

Received for publication 3 September 1991 and in final form 4 February 1992.

REFERENCES

Arnold, W. A., and R. Azzi. 1971. The mechanism of delayed light production by photosynthetic organisms and a new effect of electric fields on chloroplasts. *Photochem. Photobiol.* 14:233–240.

Avron, M. 1960. Phosphorylation by Swiss-chard chloroplasts. *Biochim. Biophys. Acta.* 40:257–272.

Blank, M., and L. Soo. 1990. Ion activation of (Na,K)-ATPase in alternating currents. *Bioelectrochem. Bioenerg.* 24:51–62.

Brumfeld, V., I. R. Miller, and R. Korenstein. 1989. Electric field-induced lateral mobility of photosystem I in the photosynthetic membrane. A study by electrophotoluminescence. *Biophys. J.* 56:607–614.

Ehrenberg, B., D. L. Farkas, E. N. Fluhler, Z. Lojewska, and L. Loew. 1987. Membrane potential induced by external electric field pulses can be followed with a potentiometric dye. *Biophys. J.* 51:833–838.

Farkas, D. L., and S. Malkin 1979. Cold storage of isolated class C chloroplasts. Optimal conditions for stabilization of photosynthetic activities. *Plant Physiol.* 60:449–451.

Farkas, D. L., R. Korenstein, and S. Malkin. 1980. Electroselection in the photosynthetic membrane: polarized luminescence induced by an external electric field. *FEBS Lett.* 120:236–242.

Farkas, D. L., R. Korenstein, and S. Malkin. 1982. Ionophore mediated ion transfer in a biological membrane: study by electrophotoluminescence. *In* Transport in Biomembranes. R. Antolini, F. A. Gliozzi, and A. Gorio, editors. Raven Press, New York. 215–226.

Farkas, D. L., R. Korenstein, and S. Malkin. 1984. Electrophotoluminescence and the electrical properties of the photosynthetic membrane. Initial kinetics and the charging capacitance of the membrane. *Biophys. J.* 45:363–373.

Farkas, D. L., S. Malkin, and R. Korenstein. 1984a. Electrophotoluminescence and the electrical properties of the photosynthetic membrane: electric field induced electrical breakdown of the photosynthetic membrane and its recovery. *Biochim. Biophys. Acta.* 767:507–514.

Gross, D., L. M., Loew, and W. W. Webb. 1986. Optical imaging of cell membrane potential changes induced by applied electric fields. *Biophys. J.* 50:339–348.

Hibino, M., M. Shigemori, H. Itoh, K. Nagayama, and K. Kinosita. 1991. Membrane conductance of an electroporated cell analyzed by submicrosecond imaging of transmembrane potential. *Biophys. J.* 59:209–220.

Kinoshita, K., I. Ashikava, N. Saita, H. Yoshimura, H. Itoh, K. Nagayama, and A. Ikegami. 1988. Electroporation of cell membrane visualized under pulsed laser fluorescence microscope. *Biophys. J.* 53:1015–1019.

Korenstein, R., D. L. Farkas, and S. Malkin. 1984. Reversible electric breakdown of swollen thylakoid membrane vesicles: study by electrophotoluminescence. *Bioelectrochem. Bioenerg.* 13:191–197.

Liu, D. S., R. D. Astumian, and T. Y. Tsong. 1990. Activation of Na^+ and K^+ pumping modes of (Na,K)-ATPase by an oscillating electric field. *J. Biol. Chem.* 265:7260–7268.

Murphy, D. J. 1986. The molecular organization of the photosynthetic membranes of higher plants. *Biochim. Biophys. Acta.* 864:33–94.

Rosemberg, Y., and R. Korenstein. 1990a. Electroporation of the photosynthetic membrane. A study by intrinsic and external optical probes. *Biophys. J.* 58:823–832.

Rosemberg, Y., and R. Korenstein. 1990b. A novel method for measuring membrane conductance changes by a voltage sensitive optical probe. *FEBS (Fed. Eur. Biochem. Soc.) Lett.* 263:155–158.

Serpersu, E. H., and T. Y. Tsong. 1983. Stimulation of a ouabain sensitive Rb^+ uptake in human erythrocytes with an external electric field. *J. Membr. Biol.* 74:191–201.

Serpersu, E. H., and T. Y. Tsong. 1984. Activation of electrogenic Rb^+ transport of (Na, K)-ATPase by electric field. *J. Biol. Chem.* 259:7155–7162.

Symons, M., S. Malkin, and R. Korenstein. 1985. External electric field effects on photosynthetic membrane vesicles: kinetic characterization of two electrophotoluminescence phases in hypotonically swollen chloroplasts. *Biochim. Biophys. Acta.* 767:223–230.

Symons, M., R. Korenstein., and S. Malkin. 1985. External electric field effects on photosynthetic vesicles. The relationship of the rapid and the slow phases of electrophotoluminescence in hypotonically swollen chloroplasts to PS I and PS II activity. *Biochim. Biophys. Acta.* 806:305–310.

Symons, M., S. Malkin, R. Korenstein, and D. L. Farkas. 1988. On the topological origin of the R and S phases of electric field induced luminescence in chloroplasts and blebs. *J. Photochem. Photobiol. B.* 1:295–303.

Tsong, T. Y., and D. Astumian. 1987. Electroconformational coupling and membrane protein function. *Prog. Biophys. Mol. Biol.* 50:1–45.

Tsong, T. Y., 1989. Deciphering the language of cells. *TIBS* 14:89–92.

Van Gorkum, H. J., R. F. Meiburg, and L. J. De Vos. 1986. Thermodynamics of the charge recombination in photosystem II. *Photosynth. Res.* 9:55–62.

Vos., M. H., and H. J. van Gorkom. 1988. Thermodynamics of electron transport in photosystem I studied by electric field-stimulated charge recombination. *Biochim. Biophys. Acta.* 934:293–302.

Vos., M. H. 1990. Electrogenic electron transport in photosynthetic systems: studies of charge recombination induced by external electric fields. Ph.D. dissertation, University of Leiden, The Netherlands.

Vos, M. H., and H. J. van Gorkom. 1990. Thermodynamical and structural information on photosynthetic systems obtained from electrophotoluminescence kinetics. *Biophys. J.* 58:1547–1555.